RECONFIGURABLE ARCHITECTURE EXTENDING BANDWIDTH LIMITS OF MICRO-ACOUSTIC RF FILTERS

Giuseppe Michetti[1] and Matteo Rinaldi[1]
[1]SMART Center, Northeastern University, MA, USA

ABSTRACT

We propose a Radio Frequency (RF) filter architecture capable of instantaneous bandwidth (BW) reconfigurability introduced by periodic modulation of single-frequency piezoelectric RF resonators. This filter topology can attain passband BW that is directly proportional to the switching frequency used to modulate the resonators, therefore exceeding the limit imposed by the piezoelectric coupling coefficient k_t^2 in conventional micro-acoustic passive filters. Moreover, the filter is based on arrays of shunted single-frequency resonators, greatly simplifying filter banks' design, representing therefore a promising candidate to meet the market demands for real-time adaptive filters with a small footprint and large BWs as required by the increasing needs of large-data rates in 5G RF mobile systems. Preliminary results are shown by using 4 commercial Surface Acoustic Waves (SAW) resonators operating at 318 MHz wire-bonded with switching dies, obtaining a 4.5 dB Insertion Loss, and tunable BW between 300kHz and 1.05kHz (3:1), paired with a 23dB out-of-band rejection.

KEYWORDS

RF MEMS; Micro-acoustic RF Filter; Reconfigurable Filter; RF Front-End; Time-Variant Network

INTRODUCTION

Micro-acoustic resonators have drawn growing attention in both industrial and academic environments for their unique performance at RF, allowing for large-scale integration of miniaturized filters, with quality factors above 1000s, for their manufacturing processes prone to large volume scaling costs, their compatibility with CMOS processing equipment and thanks to the popularization of ladder networks for RF channel duplexing[1-3].

Progress in radio frequency (RF) mobile architectures is fostered by the need for larger and larger data rates required in high-quality video streaming, as well as a growing number of interactive services are offered in mobile applications, based on real-time processed calculations, remotely prompted through RF signals available on a cellular device - a paradigm known as *cloud computing*.[4,5]

Following these trends, a constantly growing number of micro-acoustic filters is required in compact radios, stressing the technological constraints underlying the fabrication control required to synthesize the various bands on piezoelectric thin films. At the same time, frequency scaling of RF bands toward now higher data rates system constitutes the bottleneck toward the deployment of micro acoustic technologies for future radio paradigms. [6-8].

Moreover, given the lack of real-time reconfigurable components in the RF front-end chains, radio networks rely more on more on digital controls and power-hungry real-time signal RF processing techniques, mining battery lifetime, and narrowing thermal margins. [9]

Achieving tunable filter bandwidths in a compact footprint would be highly desirable to implement a true real-time, hardware-in-the-loop dynamic optimization to allow for either larger BW when the large data rate is required or lower BW to mitigate channel noise, forming a closed-loop approach to robust RF adaptive communication relaxing the role of RF digital signal processing.[10-11]

In this scenario, we proposed a novel filter architecture capable of unprecedented reconfigurability leveraging spatio-temporal modulation of RF resonators. [12-13] In this work, we further optimized the network to demonstrate a 3:1 BW large tunability introduced by means clock phase sharing between identical micro-acoustic resonators. This network, when properly actuated, breaks the conventional limits set by micro-acoustic ladder topologies, showing the capability of realizing filter with wider BWs, as well as a true real-time control on said BW through modulation control.

METHODS

Switched Filter as a Dynamic Circuit

The circuit implementing the reconfigurable filter proposed in this work is drawn in Fig.1a, and it is generally composed of N branches connecting the two RF ports. Each branch is composed of a one-port resonator, shunted to the filter ground node, that is used to transfer energy from port 1 to port 2 and vice versa.

Note that in this circuit no through component exists between the RF ports; instead, a suitable network of two switches periodically actuated with 50% duty cycle in phase opposition provides the necessary path to ground so that each resonator gets charged /discharged for 50% of the modulation period T_m. In a

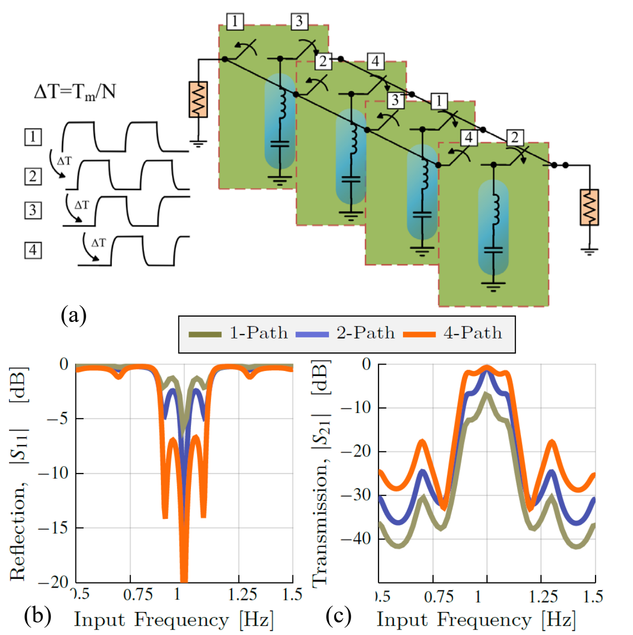

Figure 1:a) Schematic of a periodically modulated LTV filter, composed of N branches (in green shades) connecting the two RF ports through a staggered pattern of delayed ON/OFF phases. The staggering pattern is illustrated for N=4.
b) and c) represent respectively normalized reflection and transmission frequency response for 1,2 and 4 path filters composed of ideal resonators with Q_{load}=20 and actuated with $F_m=10/\tau=5/(Q_{load}\,\omega_0)$.

978-1-940470-04-7/HH2022/$25©2022TRF
DOI 10.31438/trf.hh2022.52

similar fashion to N-path filters, each branch is actuated with a delay $1/N/T_m$.

In this way, a dynamic regime of operation is induced in this circuit, implementing a specific class of circuits commonly referred to in the literature as linear-time-variant (LTV) networks. The rise-time τ of such a network can be analyzed with conventional linear-time-invariant (LTI) techniques so that it can be expressed as $\tau=2Q_{load}/\omega_0$, where Q_{load} is the external quality factor of the resonator and ω_0 its resonant frequency.

A dynamic bandpass filter regime can be achieved as shown in Fig.2(b), when such resonators are excited with modulation frequencies F_m above $1/\tau$. In this regime, energy is transferred through a mediated resonant storage mechanism as for LTI systems.

Note that for a simple one-port micro-acoustic resonator, like any other RF resonator technology, energy storage is maximized at its natural resonant frequency ω_0, so that a band-pass transfer function is achieved regardless of the technology used.

When using this LTV architecture, transmission poles required to synthesize filter passband are artificially generated at an infinite set of frequencies $Fres+kFm$. The first 2 intermodulation-induced transmission poles can be used to estimate the implemented filter bandwidth.

In other words, for this filter class:

$$BW \sim 2F_m \qquad (1)$$

Note that this BW might differ from the usual BW_{3dB} rating reported in passive filters, as the insertion loss (IL) at the band edges depends on the coupling of each resonator to the external ports, which is implemented through the switching network and therefore depends on the number of branches N used in the circuit.

To this point, it is interesting to visualize the impact of various N branches on its frequency response. Fig2(b) describes the reflection (S_{11}) and transmission (S_{21}) frequency response of a prototype filter scaled to 1Hz center frequency and with Q_{load}=20. For simplicity, S_{12} and S_{22} are not reported, given the symmetry of the circuit.

In Fig.2(b), one can see how with only 1 branch only 50% of the input energy can be passed, as the resonator is only connected to each port for 50% of T_m. Conversely, with 2 branches, all the input energy can be transferred through the resonators given the complementary actuation. At the same time, however, the passband shoulders at $F_{res}\pm F_m$ suffer from degraded IL.

Instead, when 4 branches actuated in quadrature are used the artificial poles at $F_{res}\pm F_m$ display an IL approaching the one at F_{res}, demonstrating a potential for practical use as a tunable BW passband filter. The BW achievable by this circuit is largely tunable through F_m. On the lower side, F_m is set by the inverse of the rise-time, as the resonator does not retain the input energy when $T_m >> 1/\tau$. On the higher side, the in-band ripples between the pole at F_{res} and the ones at $F_{res}\pm F_m$ increase as F_m increases, eventually exceeding the usable 3dB margin.

Micro-acoustic Switched Filter

Using one-port piezoelectric micro-acoustic resonators in this filter architecture comes with several key advantages with respect to distributed or lumped RF resonators.

For a one-port micro-acoustic resonator:

$$Q_{load} \sim \pi^2/(2\, k_t^2 \omega_0 C_0 Z_0) \qquad (2)$$

According to Eq.(2), a relatively small k_t^2 (1-10% depending on acoustic mode and piezoelectric film), ensures a relatively high Q_{load} and therefore a slower rise-time, which in turn results in fractional BW_{3dB} in the 1-10% range, requiring low-to-moderate modulation frequencies F_m (5-50MHz) for RF filters.

These attainable parameters make micro-acoustic technology an ideal candidate to deploy the LTV filter for software-defined protocols in mobile radios, where BW might be optimized in a hardware-in-the-loop type of architecture, within a compact footprint and reduced power consumption.

Resorting to a low F_m dynamic scheme leads to relaxed constraints in terms of power handling. In fact, most LTV networks implementing RF filters, such as the popular N-path filters[14-16], suffer from poor linearity under large-signal operation, as their F_m is typically comparable to the RF carrier, resulting in linearity constraints and therefore limited power handling.

Notably, when using the proposed architecture, the filter passband is not exclusively set by k_t^2, leaving room for larger achievable BWs with sufficiently high F_m. Fig.2(a) schematically demonstrates the inherent capability of this LTV filter to achieve 2-3fold larger instantaneous BW as a reference ladder filter, for the same micro-acoustic resonator k_t^2, F_{res}, Q, and C_0. On top of that, this LTV filter relies on identical resonators, whereas instead passive topologies commonly rely on close control of resonators' center frequency spacing to implement a usable passband.

This difference provides a significant advantage with respect to passive topologies, especially when frequency scaling is considered. Resonant frequency trimming of micro-acoustic devices has been pointed out in many sources as the main manufacturing bottleneck of scaling micro-acoustic filters in the mm-Wave spectrum, as well as the high bands of the 5G bands.

Lastly, as this LTV filter requires identical resonators, the usual constraints binding ladder filters' matching to 50Ω ports do not hold here, further simplifying micro-acoustic fabrication in this context.

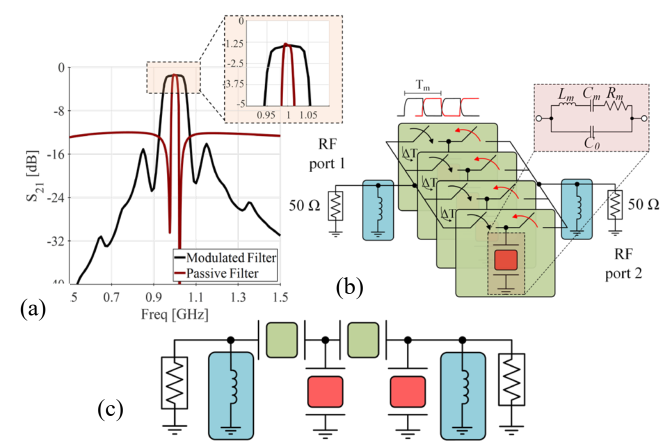

Figure 2 : a) Comparison of the transmission frequency response (S_{21}) of a 4-path micro-acoustic-based commutated LTV filter with 4 identical resonators centered at 1GHz and an equivalent conventional ladder filter composed of 4 resonators - schematics are respectively in b) and c). A typical model of a piezoelectric micro-acoustic resonator is sketched in the red inset of b). For both simulations, micro-acoustic technology using k_t^2=5% and Q=1k was employed. The LTV topology is modulated at a fractional F_m=0.05F_{res}. As noted in a), the LTV topology can implement much broader transmission BW for the same IL.

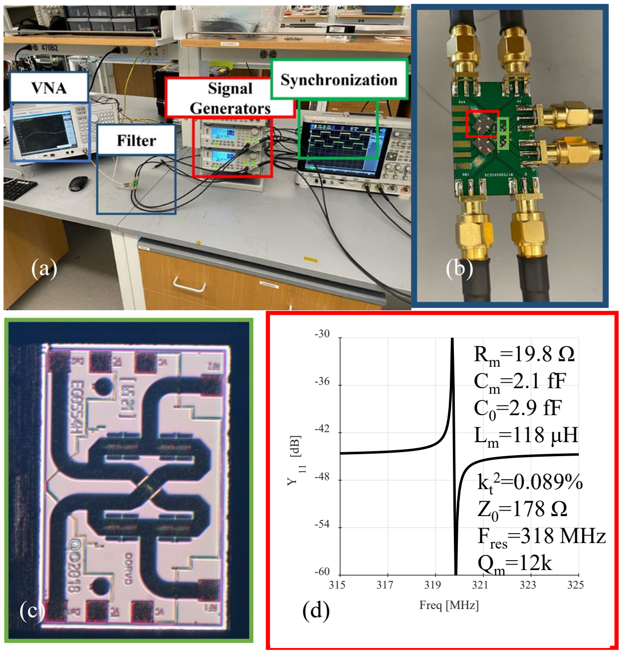

Figure 4: (a) Overview of the experimental setup used to characterize the LTV filter response, composed of two signal generators, synchronized in closed loop via MATLAB interface. The 4 modulation signals are fed to a custom PCB (in (b)) and the circuit is interfaced with two RF ports via coax cables. Scattering parameters are measured via a Keysight VNA as F_m is varied programmatically. In (c), a micrograph picture of the QORVO™ DPDT RF switch deployed in this experiment. In (d), a fitted response of the RFMI™ SAW resonators used in this demo and die attached to the PCB in (b).

RESULTS

An early-stage experimental demonstration is designed to address the filter performance with real micro-acoustic resonator components. A lab experimental setup is remotely programmed via MATLAB to acquire filter frequency response, across a sweep of modulation frequencies F_m. Accordingly to Eq.(2) an F_m range between 50 kHz and 300 kHz is selected.

RFMI™ packaged SAW resonators are selected as off-the-shelf components for this filter(Fig.4d), operating at F_{res}=318 MHz, with k_t^2=0.089%, C_0=2.9pF (corresponding to 172Ohm), and Q_m=12k and die attached to a custom PCB.

An off-the-shelf couple of QORVO™ Double-Pole-Double-Through (DPDT) die RF switch(Fig.4c) is die-attached to a custom PCB(Fig.4b), and the RF pins are wire-bonded to the SAW leads to implement a 4-path micro-acoustic switched filter**.**

Two couples of complementary modulation signals are generated in quadrature by using two TSG3152 TTI™ signal generators, and ultimately fed on the DPDT controls on the PCB. RF response is measured on a Keysight VNA and recorded programmatically as F_m is varied (Fig.1a).

Despite the high Q_m of the SAW, calculated motional resistance R_m approaches 20Ω due to extremely poor k_t^2, overall limiting the measured IL to circa 5dB (Fig.4a-b). and resulting in extremely narrowband operation between 300kHz and 1.05MHz.

Moreover, from Fig.4(a-b) the filter sidelobes follow the F_m scaling law discussed in the Methods, essentially confirming the predicted trends, and proving feasible real-time BW tunability without resorting to passive tunable components.

Linearity performance is measured using an RF power amplifier fed by a sinusoidal excitation at the filter center frequency (318MHz) resulting in a *P_{1dB}=13.5dBm*.

A comparison between the measured performance for the LTV switched filter and for an equivalent ladder filter can be drawn if it is assumed, for the ladder filter. that the same resonator performance in terms of Q_m, k_t^2 can be achieved when F_{res} and C_0 are properly scaled to satisfy the requirements to obtain a ladder-type filter response (for example, following the design guidelines explained in [17]**.**)

When directly comparing the two responses, the measured LTV filter outperforms ladder filter BW by a factor of 3 (0.1% vs 0.033%) and displays a lower IL (8.4dB vs 4.5dB), despite nonidealities for ladder filter have not being accounted for.

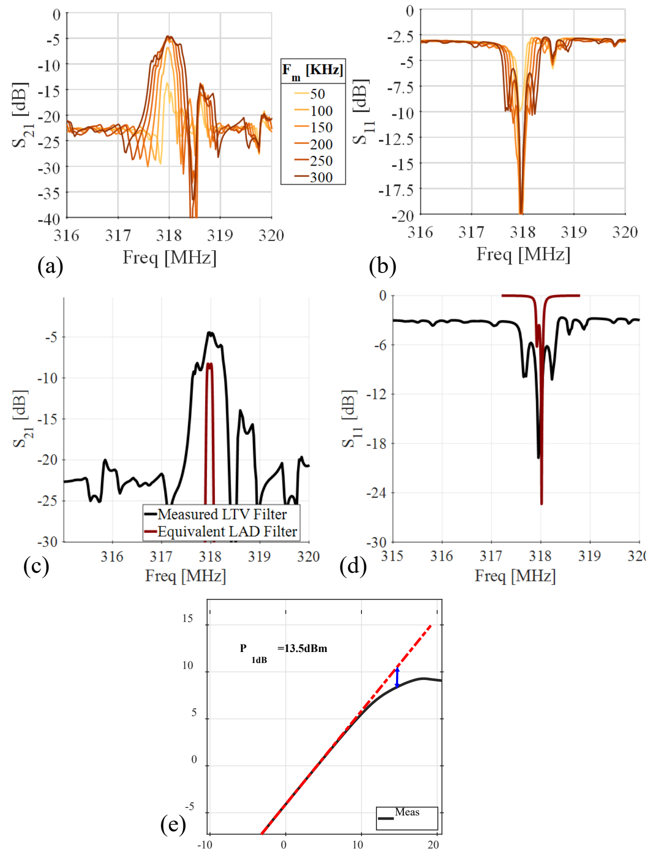

Figure 5: (a-b) Experimental results from the setup in Fig.3, in terms of transmission parameters (S_{21}) and reflection parameters (S_{11}) for various modulation frequencies F_m . Small fractional F_m correspond to achieved BW ranging from 0.03% to 0.1% for a peak IL of 4.5dB, mostly due to the poor k_t^2 of the SAW resonators. Approximately 0.5dB IL is attributed to 5Ω R_{ON} of said DPDT Switches, while 4dB IL is attributed to 20Ω R_m of the SAWs. (Fig.3b). (c-d) Comparison of experimental LTV filter response with equivalent ladder filter implemented with resonator parameters from Fig.3b. The BW enhancement introduced by the LTV network is 3.3-fold with respect to the passive ladder network realized with the same technology. Moreover, the LTV filter exhibits lower IL given the same C_0,Q,k_t^2, for this narrowband filter design. (e) measured linearity of 13.5dBm, limited by the SAW power handling (as the DPDT power handling approaches 28dBm).

CONCLUSIONS

Despite the low absolute BW demonstrated in this experiment, due to the choice of off-the-shelf SAW resonator components, a filter architecture that can exceed the BW limits posed by the resonator k_t^2 has been proposed, modeled, and experimentally demonstrated in this work.

Details of micro-acoustic RF filter operation have been introduced to provide rule-of-thumb design guidelines for the interested filter designers, and clear comparisons have been provided to show that the filter indeed exceeds most performance of conventional ladder filters.

Moreover, a micro-acoustic RF filter with a native tunability has been presented and experimentally validated, with a unique BW tuning capability exceeding 5 to 1 without the need for tunable components but relying instead on a reconfigurable switching network.

REFERENCES

[1] T. Matsumura, M. Esashi, H. Harada and S. Tanaka, "Multi-band RF filter integrating different modes of AlN resonator by CMOS-compatible process," *2009 IEEE International Ultrasonics Symposium*, 2009, pp. 2141-2144, doi: 10.1109/ULTSYM.2009.5442012.

[2] R. Aigner, J. Ella, H. -. Timme, L. Elbrecht, W. Nessler and S. Marksteiner, "Advancement of MEMS into RF-filter applications," *Digest. International Electron Devices Meeting,*, 2002, pp. 897-900, doi: 10.1109/IEDM.2002.1175981.

[3] R. Ruby, "The 'how & why' a deceptively simple acoustic resonator became the basis of a multi-billion dollar industry," *2017 IEEE 30th International Conference on Micro Electro Mechanical Systems (MEMS)*, 2017, pp. 308-313, doi: 10.1109/MICRO-ACOUSTICYS.2017.7863403.

[4] F. Boccardi, R. W. Heath, A. Lozano, T. L. Marzetta and P. Popovski, "Five disruptive technology directions for 5G," in IEEE Communications Magazine, vol. 52, no. 2, pp. 74-80, February 2014, doi: 10.1109/MCOM.2014.6736746.

[5] L. Larson, "Rf and Microwave Hardware Challenges for Future Radio Spectrum Access," Proceedings of the IEEE, vol. 102, no. 3, pp. 321–333, 2014.

[6] S. Mahon, "The 5G Effect on RF Filter Technologies," in *IEEE Transactions on Semiconductor Manufacturing*, vol. 30, no. 4, pp. 494-499, Nov. 2017, doi: 10.1109/TSM.2017.2757879.

[7] W. J. Chappell, E. J. Naglich, C. Maxey and A. C. Guyette, "Putting the Radio in "Software-Defined Radio": Hardware Developments for Adaptable RF Systems," in Proceedings of the IEEE, vol. 102, no. 3, pp. 307-320, March 2014, doi: 10.1109/JPROC.2014.2298491.

[8] J. Mitola, "Cognitive Radio Architecture Evolution," in *Proceedings of the IEEE*, vol. 97, no. 4, pp. 626-641, April 2009, doi: 10.1109/JPROC.2009.2013012.

[9] J. Mueller *et al*., "Requirements for reconfigurable 4G front-ends," *2013 IEEE MTT-S International Microwave Symposium Digest (MTT)*, 2013, pp. 1-4, doi: 10.1109/MWSYM.2013.6697534.

[10] H. H. Sigmarsson, J. Lee, D. Peroulis and W. J. Chappell, "Reconfigurable-order bandpass filter for frequency agile systems," 2010 IEEE MTT-S International Microwave Symposium, 2010, pp. 1756-1759, doi: 10.1109/MWSYM.2010.5518024.

[11] E. Schmidhammer, T. Metzger and C. Hoffmann, "Multiplexers: A necessary extension for 4G/5G systems," 2016 IEEE MTT-S International Microwave Symposium (IMS), 2016, pp. 1-4, doi: 10.1109/MWSYM.2016.7540222.

[12] G. Michetti, M. Pirro, Y. Yu, G. Chen, C. Cassella and M. Rinaldi, "Reconfigurable N-Path MEMS Filter Based on the Periodic Commutation of Single Frequency Resonators," 2020 IEEE 33rd International Conference on Micro Electro Mechanical Systems (MEMS), 2020, pp. 1274-1277, doi: 10.1109/MEMS46641.2020.9056403.

[13] G. Michetti, A. Mekawy, L. Colombo, M. Pirro, A. Alù and M. Rinaldi, "Filter Architecture Operating Beyond the Q Limit and With Real-Time Bandwidth Tunability," *2021 IEEE MTT-S International Microwave Filter Workshop (IMFW)*, 2021, pp. 218-220, doi: 10.1109/IMFW49589.2021.9642298.

[14] A. Ghaffari, E. A. M. Klumperink, M. C. M. Soer and B. Nauta, "Tunable High-Q N-Path Band-Pass Filters: Modeling and Verification," in IEEE Journal of Solid-State Circuits, vol. 46, no. 5, pp. 998-1010, May 2011, doi: 10.1109/JSSC.2011.2117010.

[15] A. E. J. Ng and J. I. Sewell, "N-path and pseudo-N-path cells for switched-current signal processing," in *IEEE Transactions on Circuits and Systems II: Analog and Digital Signal Processing*, vol. 46, no. 9, pp. 1148-1160, Sept. 1999, doi: 10.1109/82.793705.

[16] K. Kibaroglu and G. M. Rebeiz, "An N-path bandpass filter with a tuning range of 0.1–12 GHz and stopband rejection > 20 dB in 32 nm SOI CMOS," 2016 IEEE MTT-S International Microwave Symposium (IMS), 2016, pp. 1-3, doi: 10.1109/MWSYM.2016.7539982.

[17] s. Menendez, P. de Paco, R. Villarino and J. Parron, "Closed-Form Expressions for the Design of Ladder-Type FBAR Filters," in *IEEE Microwave and Wireless Components Letters*, vol. 16, no. 12, pp. 657-659, Dec. 2006, doi: 10.1109/LMWC.2006.885610.

CONTACT

*G.Michetti, michetti.g@northeastern.edu